HAL
open science

From steep-slope volcano to flat caldera floor

Stéphanie Barde-Cabusson, Olivier Merle

To cite this version:

Stéphanie Barde-Cabusson, Olivier Merle. From steep-slope volcano to flat caldera floor. Geophysical Research Letters, 2007, 34, pp.L10305. 10.1029/2007GL029784 . hal-00327966

HAL Id: hal-00327966

https://hal.science/hal-00327966v1

Submitted on 26 May 2021

HAL is a multi-disciplinary open access archive for the deposit and dissemination of scientific research documents, whether they are published or not. The documents may come from teaching and research institutions in France or abroad, or from public or private research centers.

L'archive ouverte pluridisciplinaire **HAL**, est destinée au dépôt et à la diffusion de documents scientifiques de niveau recherche, publiés ou non, émanant des établissements d'enseignement et de recherche français ou étrangers, des laboratoires publics ou privés.

From steep-slope volcano to flat caldera floor

Stéphanie Barde-Cabusson[1] and Olivier Merle[1]

Received 22 February 2007; revised 2 April 2007; accepted 17 April 2007; published 23 May 2007.

[1] Most laboratory experiments of caldera collapse have dealt with reservoir emptying below a flat-lying overburden without an overlying analogue volcanic edifice on top. The overload and the role of topography are then neglected so that the final flat floor within the caldera is directly linked to the initial one. In addition, caldera subsidence is commonly attributed to the collapse of the top of a magma chamber linked to eruptions delivering large amounts of volcanic products. Analogue experiments show that the deformation of a weak clay-rich core resulting from the hydrothermal alteration in a volcanic edifice can, in certain conditions, reproduce the structures of a caldera. In particular, it is a way to explain the flat floor of a caldera when resurfacing resulting from new eruptions or destructive processes seems unlikely. **Citation:** Barde-Cabusson, S., and O. Merle (2007), From steep-slope volcano to flat caldera floor, *Geophys. Res. Lett.*, *34*, L10305, doi:10.1029/2007GL029784.

1. Caldera Formation

[2] Caldera formation is commonly associated with eruption of volcanic products and attributed to the collapse of the roof of a reservoir resulting from magma withdrawal. This can result either from a single eruption draining efficiently a huge volume of magma or from recurrent eruptions and multiple dyking events leading to an incremental or step by step collapse of the reservoir [e.g., *Lipman*, 1997; *Munro and Rowland*, 1996]. Whatever the models, the collapsed surface corresponds approximately to the dimensions of the underlying reservoir.

[3] In some cases, geophysical data together with field data show that there is not a reservoir large enough to permit such a collapse. For example, the classic caldera model is unlikely for the Enclos Caldera at Piton de la Fournaise on Reunion Island [e.g., *Rousset et al.*, 1989; *Nercessian et al.*, 1996; *Briole et al.*, 1998; *Malengreau et al.*, 1999] or on the French Polynesia Island of Nuku Hiva [*Legendre et al.*, 2005; *Maury et al.*, 2005].

[4] Hot fluid circulation of both groundwater and magmatic gas deeply alters volcanic rock and produce volume loss together with clay-rich zones able to flow under their own weight. Recent studies have shown that such altered rocks form large zones within edifices and initiate sector collapses [*López and Williams*, 1993; *Day*, 1996; *Vallance and Scott*, 1997; *Voight and Elsworth*, 1997; *van Wyk de Vries et al.*, 2000; *Reid et al.*, 2001; *Cecchi et al.*, 2005]. Also, the core of the volcano may become unstable if conditions of weak lateral confinement exist at the boundary of the hydrothermal system, which then flows laterally. The ensuing collapse of the central part of the edifice may then create a caldera-like structure apparently similar to classical calderas but named "caldera-like" as the drained material is not magma but altered rock [*Merle and Lénat*, 2003; *Merle et al.*, 2006].

2. Caldera Floor Topography

[5] The classic image of a caldera structure is that of a huge cauldron with a flat floor surrounded by a ring fault exhibiting a circular vertical cliff of several hundred meters high. The question is rarely asked as to how and by which mechanism such a flat floor can form starting from a steep-slope cone. Many young caldera structures are filled by thick volcanic sequences and rare are those that are eroded to the original surface. Very little evidence is thus available to evaluate the degree of disruption of the floor and the initial intra-caldera slopes.

[6] Concerning previous experimental studies on caldera formation, only recent studies took the initial topography of a volcanic cone into account. Using a cone with a slope of 10° and a flattened apex, *Troll et al.* [2002] describe both piecemeal subsidence as a consequence of inflation and deflation of the chamber and piston subsidence linked to simple chamber emptying, but the final topography is not described. *Walter and Troll* [2001] outline, in experiments of chamber deflation under a cone, an initial apical sagging and a tilt of the flanks until a delayed bench-like collapse of the caldera floor. *Lavallée et al.* [2004] points out the problem of initial topography in scaled physical models and illustrates the real influence of pre-existing relief upon the style of caldera subsidence due to magma withdrawal.

[7] In this paper, we investigate experimentally the formation of caldera-like structures resulting from the ductile flow of very large hydrothermal systems. As opposed to previous experiments on that matter [*Merle and Lénat*, 2003; *Merle et al.*, 2006], no reduction of lateral stresses to trigger or speed up the collapse process is introduced in the experimental procedure. We pay special attention to the slope modification of the initial cone during the deformation.

3. Experimental Procedure

[8] In many previous experiments on caldera formation, the reservoir was simulated using a balloon or a bladder filled with air or water and buried within a cohesive material [*Kennedy et al.*, 2004; *Lavallée et al.*, 2004; *Holohan et al.*, 2005]. Sometimes, viscous materials like golden syrup, silicone or dry ice are directly emplaced into the cohesive material [*Komuro*, 1987; *Acocella et al.*, 2000; *Roche et al.*, 2000]. In some experiments, inflation of the balloon predates deflation to simulate a complete process from magma arrival to magma emptying. In experiments conducted here,

[1]Laboratoire Magmas et Volcans, Observatoire de Physique du Globe de Clermont-Ferrand, Clermont-Ferrand, France.

Copyright 2007 by the American Geophysical Union.
0094-8276/07/2007GL029784

Table 1. Parameters

Variable	Definition	Nature	Model
B	Diameter of the cone	5–30 km	5–30 cm
D	Diameter of the ductile core	1–15 km	1–15 cm
H	Offset along the normal fault	1–2 km	1–2 cm
h	Height of the brittle cone	1–3 km	1–3 cm
$\varnothing$	Angle of friction	33°–37°	33°–37°
g	Gravitational acceleration	9.81 m/s^2	9.81 m/s^2
ρ_v	Density of the brittle cone	2500 kg m^{-3}	1300 kg m^{-3}
ρ_h	Density of the ductile core	1600 kg m^{-3}	1000 kg m^{-3}
τ_0	Cohesion	10^7 Pa	50 Pa
t	Time span for caldera formation	300 y	1 h
η	Viscosity of the ductile core	10^{16} Pa.s	5×10^4 Pa.s

the goal is to investigate the effect of a low-strength zone simulating the hydrothermal system localised in the core of a cohesive edifice and no inflation process has to be simulated.

[9] The experimental setup consists of a piece of silicone upon which a steep-slope cone of cohesive material is built. A layering of different colours helps to highlight the structures after deformation. The diameter of the cone is in the range from 5 to 30 cm (i.e., 5 to 30 km in nature) and its slope is about 30 degrees. The internal structure is observed via cross-sections cut through the models after deformation. The topography of the analogue model is preserved by pouring new sand on top of the model, which is then wet with water, to make possible to cut cross-sections in the solidified model.

4. Scaling

[10] The clay-rich altered core is considered to behave as a viscous fluid and is simulated by silicone putty emplaced in the central part of the analogue model [e.g., *van Wyk de Vries et al.*, 2000]. The brittle part of the edifice is simulated by a dry sand/plaster mixture as in most analogue experiments on volcano deformation [e.g., *Donnadieu and Merle*, 1998].

[11] The shape of hydrothermal systems is poorly known as their boundaries have no sharp limits and are difficult to image accurately via geophysical approaches. When studying the geo-electrical model of the central part of Piton de la Fournaise volcano, *Lénat et al.* [2000] detected the upper limit of a zone of low conductivity (0–20 ohm.m) in the Enclos caldera inferred to be the hydrothermal system. The overall shape of the zone mimics a low-slope cone. From this information and to simplify the experimental procedure, we choose to test both conical and cylindrical shape ductile structures in our experiments.

[12] Similarity conditions are achieved through a set of Π dimensionless numbers [see *Merle and Borgia*, 1996], which must be of the same order of magnitude in nature and experiments (Tables 1 and 2). The Reynolds number is the only one to be different in nature and experiments. However, the very small values of Π_6 (10^{-17} in nature and 10^{-10} in experiments) show that the inertial forces are negligible with respect to the viscous forces both in nature and experiments. Thus, this number need receive no further consideration.

5. Results

[13] A control experiment has first been carried out where a piece of silicone was buried into a pile of horizontal sand layers. Such a configuration is perfectly stable and no deformation can be observed.

[14] A set of experiments with a 30°-slope cone has then been conducted varying the shape and thickness of the silicone. These experiments do not reveal notable differences in the whole deformation process, even when using a slightly conical or a cylindrical piece of silicone, so that all following experiments have been done with a low to medium height-to-diameter ratio cylinder (Figure 1). Subsequently, cone slope variation has been tested.

[15] The most informative experiments are those built with steep-slope cones (>25°). Deformation starts instantaneously and reveals three successive stages. The first one corresponds to rapid flattening on top of the cone without lateral bulging. This deflation stage delimits a large upper flat area. This is the major change of the shape of the analogue volcano observed during the whole duration of the experiment. The second stage corresponds to the progressive appearance of a circular ring fault surrounding the flat zone formed previously. The third and last stage is associated with the collapse of the flat zone along the ring fault, leading to a caldera-like structure. Its topography contrasts remarkably with the undisturbed external slopes of the cone (Figure 2). A slight steepening of these external slopes is sometimes observed next to the ring fault during the caldera-like formation and may generate local sector collapses.

[16] Cross-sections reveal that the brittle cone has flattened without any internal faults or fractures. The shape of the silicone has evolved with time and the initially

Table 2. The 7 Dimensionless Numbers

Definition	Calculation	Nature	Model
Geometric ratios	$\Pi_1 = \frac{B}{D}$	5.2	5–2
$\Longleftrightarrow$ scale 1 km = 1 cm	$\Pi_2 = \frac{H}{D}$		1–1.3
		Brittle material	
Angle of friction	$\Pi_3 = \phi$	33°–37°	33°–37°
Gravitational stress/cohesion	$\Pi_4 = \frac{\rho_v g h}{\tau_0}$	2.5–7.3	2.6–7.7
		Ductile material	
Gravitational force/viscous force	$\Pi_5 = \frac{\rho_h g h t}{\eta}$	14.8–44.5	7–21.2
Reynolds number	$\Pi_6 = \frac{\rho_h h^2}{\eta t}$	$1.7 \times 10^{-17} - 1.5 \times 10^{-16}$	$5.6 \times 10^{-10} - 5 \times 10^{-9}$
Density ratio	$\Pi_7 = \frac{\rho_v}{\rho_h}$	1.5	1.3

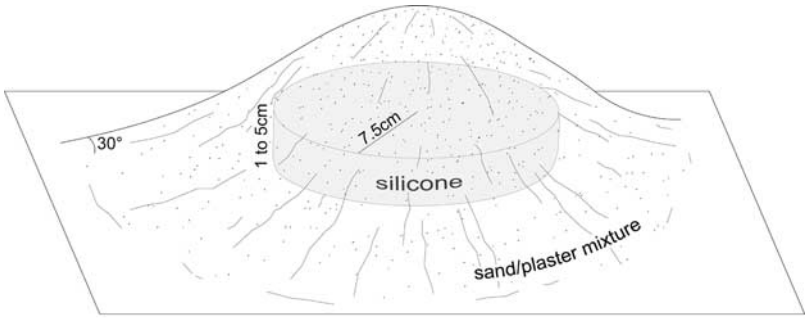

Figure 1. Sketch of the model. A ductile core of silicone is embedded into a brittle cone.

horizontal or convex upper limit has become concave downward, centered below the former summit of the cone. The ring fault outlines the circular edge of the silicone, which has intruded upward within the fracture, up to the surface in some experiments (Figure 2).

[17] Other experiments have been conducted diminishing the slope of the overlying cone. The deformation starts more slowly than in steep-slope experiments and may not reach the formation of a caldera-like structure. With slopes less than 15 degrees, a slight depression forms on top of the analogue volcano and no ring fault can be detected. When slopes are nearly flat, no deformation occurs. This indicates that the slope of the cone has a major influence on the deformation process.

[18] Decreasing the thickness of the silicone leads to a smaller offset along the ring fault as less ductile material can flow underneath. The deformational process can even be inhibited when there is not enough silicone to allow ductile flow.

6. Interpretation

[19] Given the lack of deformation for a flat topography, it appears that the formation of a caldera-like structure is due to the presence of a cone above a ductile body and is dependant upon the boundary conditions along the edge of this body. The distribution of the load (ρgh) above the silicone is not uniform and a radial and horizontal

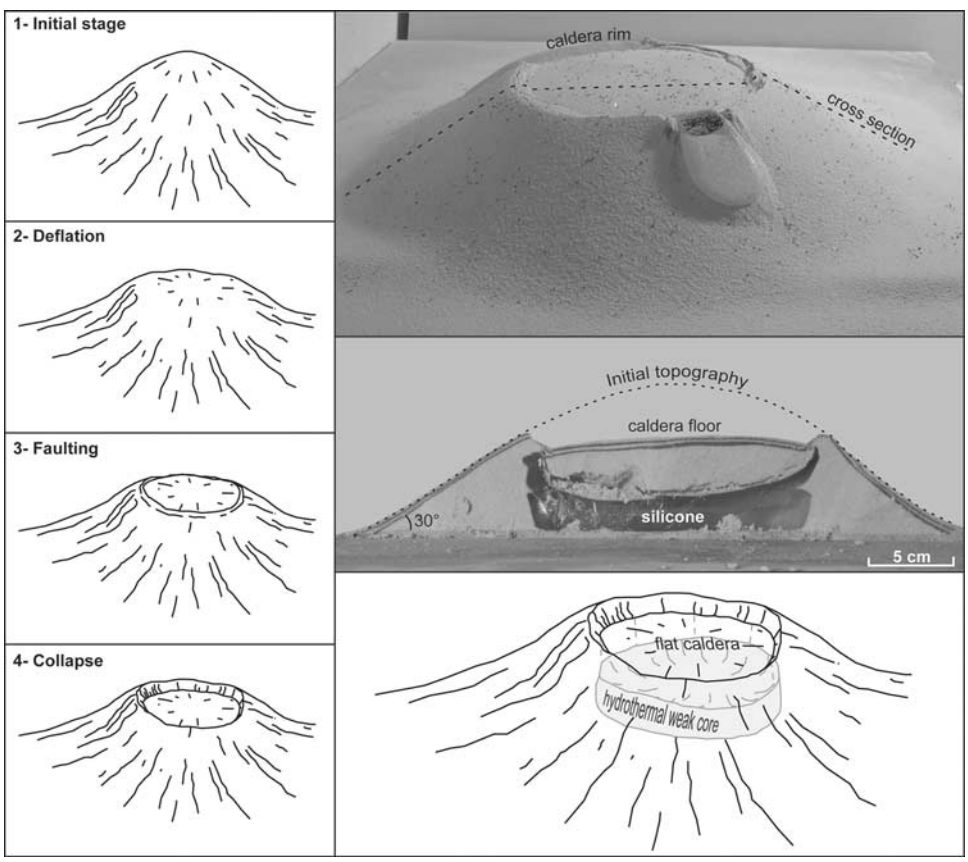

Figure 2. Caldera-like formation. Summit flattening (stage 2) occurs early and is followed by the formation of the ring fault (stage 3) along which collapse takes place (stage 4). Photographs of both panoramic and cross-section views reveal a flat caldera-like floor surrounded by steep slopes.

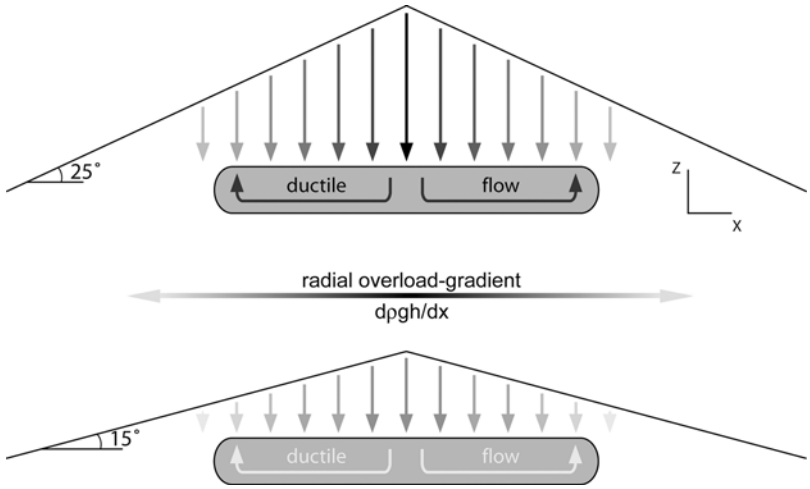

Figure 3. Load distribution above the weak zone. In steep slope (>25°) experiments, the high overburden gradient in the *x* direction allows the upward ductile flow along the edge to overcome the strength of the overlying brittle material, which does not occur with gentle slope (<15°) experiments.

overburden gradient, ($d\rho gh/dx$, Figure 3), is evidenced from high loading at the centre of the silicone, that is under the summit of the cone, to low loading along the edges. This radial gradient promotes the deformation of the silicone that narrows in the centre due to the weight of the summit of the cone and flows laterally to the low overloaded edges. This ductile deformation is accompanied by the subsidence of the upper part of the cone, which forms the upper flat area. It is noteworthy that the flat floor is formed before the onset of the caldera-like collapse.

[20] Further deformation is dependant on the intensity of the overburden gradient. With low slopes (i.e., low overburden gradient), the deformation may stop and the evolution to the formation of a caldera-like structure does not occur. With steep slopes (i.e., high gradient), the silicone that is blocked laterally by the analogue volcano flank may overcome the vertical overburden, which is relatively low there, and start to rise up. At the surface, this stage is associated with the initiation of the ring fault that foreshadows the collapse. However, offset remains limited at this stage as, very much like classic calderas, a real collapse of the roof requires enough drainage of the ductile material. For this to occur, the hydrothermal zone must be large enough and as close to the surface as possible, which permits the overburden resistance to be overcome. Then, the altered rock of the hydrothermal system would be squeezed upward along the edges, enlarging the ring fault, which is unrecognisable at depth (cross-section in Figure 2) and causing the slight slope increase next to the ring fault. In most experiments, the silicone pierces the surface along the ring-fault, and flows slowly downward (Figure 2). Such emptying of the ductile body is very efficient and speeds up the caldera-like collapse.

[21] In experiments, the silicone flows as a viscous material when reaching the surface. This is a limitation of the analogue modelling, which cannot reproduce the rheol-

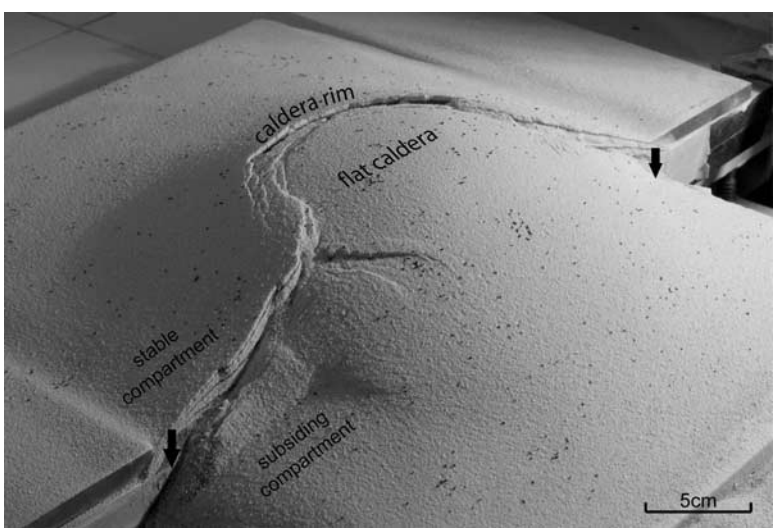

Figure 4. Complementary gentle slopes (<15°) experiment. Weak lateral confinement is achieved from normal faulting lowering part of the edifice. The same three successive stages of deflation, faulting, and collapse as shown in Figure 2 are observed with time.

ogy changes probably sustained by the hydrothermally altered rock during its rise and cooling along the ring fault. In nature, rather than a viscous flow, it would appear at the surface as a mix of breccias and clay in variable proportions.

[22] Locating the ductile body below a certain depth, that is below the base of the volcano, inhibits the process as the cone effect becomes too low to trigger deformation. To a very good approximation, a ductile body deeply buried under the base of the volcano makes the experimental conditions identical to that of the control experiment.

[23] In a complementary experiment, the effect of a fault lowering part of a volcano has been tested, according to the process proposed by *Merle et al.* [2006]. They studied the formation of the caldera-like structure on Nuku Hiva Island, supposed to result from weak lateral confinement of the hydrothermal system. The authors used simplified models, with flat-lying topography, to demonstrate the consistency of the model. When using a low-slope cone instead of a flat topography, the three successive stages described above can again be observed. Firstly, the summit of the cone flattens at the onset of the deformation to form a large upper flat area. Secondly, slow subsurface lateral spreading of the silicone initiates a ring fault. Thirdly, collapse occurs along the ring fault to form a caldera-like structure breached on one side (Figure 4). This suggests that the general process described here may happen in different tectonic environments and takes place once the ductile body inside the volcano can easily be deformed.

7. Conclusions

[24] In the situation of caldera-like formation by ductile deformation of the hydrothermal system, experiments show that the flat floor forms early by summit flattening before the formation of the ring fault along which the collapse occurs. This happens only when the hydrothermal system of the volcano can deform within the volcano to modify the natural equilibrium between ductile altered rock and brittle overburden on the edges of the system. Experiments shown here are scaled for the deformation of a clay-rich core and do not apply to the formation of a classic caldera by emptying of a magmatic reservoir. However, it cannot be ruled out that the process of flat floor caldera-like formation is similar to that of a classic caldera, given that the rheology of the whole system is very close, composed of a viscous reservoir able to flow surmounted by a pile of brittle volcanic rocks.

[25] **Acknowledgments.** We thank Valerio Acocella and an anonymous reviewer for useful reviews of the manuscript.

References

Acocella, V., F. Cifelli, and R. Funiciello (2000), Analogue models of collapse calderas and resurgent domes, *J. Volcanol. Geotherm. Res.*, *104*, 81–96.

Briole, P., P. Bachèlery, B. McGuire, J. Moss, J. C. Ruegg, and P. Sabourault (1998), Deformation of Piton de la Fournaise: Evolution of the monitoring techniques and knowledge acquired in the last five years, in *Proceedings, 2nd Workshop on European Laboratory Volcanoes, Santorini, Greece, 1996*, edited by R. Casale et al., pp. 467–474, Eur. Comm., Brussels.

Cecchi, E., B. van Wyk de Vries, and J.-M. Lavest (2005), Flank spreading and collapse of weak-cored volcanoes, *Bull. Volcanol.*, *67*, 72–91.

Day, S. J. (1996), Hydrothermal pore fluid pressure and the stability of porous, permeable volcano, *Geol. Soc. Spec. Publ.*, *110*, 77–93.

Donnadieu, F., and O. Merle (1998), Experiments on the indentation process during cryptodome intrusion: New insights into Mt. St. Helens deformation, *Geology*, *26*, 79–82.

Holohan, E. P., V. R. Troll, T. R. Walter, S. Münn, S. McDonnell, and Z. K. Shipton (2005), Elliptical calderas in active tectonic settings: An experimental approach, *J. Volcanol. Geotherm. Res.*, *144*, 119–136.

Kennedy, B., J. Stix, J. W. Vallance, Y. Lavallée, and M.-A. Longpré (2004), Controls on caldera structure: Results from analogue sandbox modeling, *Geol. Soc. Am. Bull.*, *116*, 515–524.

Komuro, H. (1987), Experiments on cauldron formation: A polygonal cauldron and ring fractures, *J. Volcanol. Geotherm. Res.*, *31*, 139–149.

Lavallée, Y., J. Stix, B. Kennedy, M. Richer, and M.-A. Longpré (2004), Caldera subsidence in areas of variable topographic relief: Results from analogue modeling, *J. Volcanol. Geotherm. Res.*, *129*, 219–236.

Legendre, C., R. C. Maury, D. Savanier, J. Cotten, C. Chauvel, C. Hémond, C. Bollinger, G. Guille, S. Blais, and P. Rossi (2005), The origin of intermediate and evolved lavas in the Marquesas archipelago: An example from Nuku Hiva island (Marquesas, French Polynesia), *J. Volcanol. Geotherm. Res.*, *143*, 293–317.

Lénat, J.-F., D. Fitterman, D. B. Jackson, and P. Labazuy (2000), Geoelectrical structure of the central zone of Piton de la Fournaise volcano (Réunion), *Bull. Volcanol.*, *62*, 75–89.

Lipman, P. W. (1997), Subsidence of ash-flow calderas: Relation to caldera size and magma chamber geometry, *Bull. Volcanol.*, *59*, 198–218.

López, D. L., and S. N. Williams (1993), Catastrophic volcanic collapse: Relation to hydrothermal processes, *Science*, *260*, 1794–1796.

Malengreau, B., J.-F. Lénat, and J.-L. Froger (1999), Structure of Réunion Island (Indian Ocean) inferred from the interpretation of gravity anomalies, *J. Volcanol. Geotherm. Res.*, *88*, 131–146.

Maury, R. C., G. Guille, C. Legendre, D. Savanier, H. Guillou, P. Rossi, and S. Blais (2005), Notice explicative, carte géologique de la France (1/50000), feuille de Nuku Hiva, Polynésie française, BRGM Éd., Orléans, France.

Merle, O., and A. Borgia (1996), Scaled experiments on volcanic spreading, *J. Geophys. Res.*, *101*(B6), 13,805–13,817.

Merle, O., and J.-F. Lénat (2003), Hybrid collapse mechanism at Piton de la Fournaise volcano, Réunion Island, Indian Ocean, *J. Geophys. Res.*, *108*(B3), 2166, doi:10.1029/2002JB002014.

Merle, O., S. Barde Cabusson, R. C. Maury, C. Legendre, G. Guille, and S. Blais (2006), Caldera core collapse triggered by regional faulting, *J. Volcanol. Geotherm. Res.*, *158*, 269–280.

Munro, D. C., and S. K. Rowland (1996), Caldera morphology in the western Galápagos and implications for volcano eruptive behavior and mechanisms of caldera formation, *J. Volcanol. Geotherm. Res.*, *72*, 85–100.

Nercessian, A., A. Hirn, J.-C. Lepine, and M. Sapin (1996), Internal structure of Piton de la Fournaise volcano from seismic wave propagation and earthquake distribution, *J. Volcanol. Geotherm. Res.*, *70*, 123–143.

Reid, M. E., T. W. Sisson, and D. L. Brien (2001), Volcano collapse promoted by hydrothermal alteration and edifice shape, Mount Rainier, Washington, *Geology*, *29*(9), 779–782.

Roche, O., T. H. Druitt, and O. Merle (2000), Experimental study of caldera formation, *J. Volcanol. Geotherm. Res.*, *105*, 395–416.

Rousset, D., A. Lesquer, A. Bonneville, and J.-F. Lénat (1989), Complete gravity study of Piton de la Fournaise volcano, Réunion, *J. Volcanol. Geotherm. Res.*, *36*, 37–52.

Troll, V. R., T. R. Walter, and H.-U. Schmincke (2002), Cyclic caldera collapse: Piston or piecemeal subsidence? Field and experimental evidence, *Geology*, *30*(2), 135–138.

Vallance, J. W., and K. M. Scott (1997), The Osceola mudflow from Mont Rainier: Sedimentology and hazard implications of a huge clay-rich debris flow, *Geol. Soc. Am. Bull.*, *109*, 143–163.

van Wyk de Vries, B., N. Kerle, and D. Petley (2000), Sector collapse forming at Casita volcano, Nicaragua, *Geology*, *28*(2), 167–170.

Voight, B., and D. Elsworth (1997), Failure of volcano slope, *Géotechnique*, *47*(1), 1–31.

Walter, T. R., and V. R. Troll (2001), Formation of caldera periphery faults: An experimental study, *Bull. Volcanol.*, *63*, 191–203.

S. Barde-Cabusson and O. Merle, Laboratoire Magmas et Volcans, Observatoire de Physique du Globe de Clermont-Ferrand, 5 rue Kessler, F-63038 Clermont-Ferrand, France. (s.bardecabusson@opgc.univ-bpclermont.fr)